GSA Data Repository 2017356

Gothmann et al., 2017, A Cenozoic record of seawater Mg isotopes in well-preserved fossil corals: Geology, doi:10.1130/G39418.1.

EXTENDED METHODS:

Samples

Additional details regarding fossil coral sample provenance and identification can be found in Gothmann et al. (2015). The fossil coral samples studied here were screened for diagenesis using x-ray diffractometry, scanning electron microscopy, petrographic microscopy, cathodoluminescence microscopy, micro-raman spectroscopy, $^{87}Sr/^{86}Sr$ measurements, carbonate clumped isotope thermometry, and Secondary Ion Mass Spectrometry (SIMS) measurements of trace elements sensitive to diagenesis (Gothmann et al., 2015).

Separation Chemistry

For the traditional ion-exchange separation method used for isolating Mg, dissolved coral samples were dried down and loaded onto a column filled with BioRad X12 resin. Mg and alkali metals including Na and K were eluted with 9N HCl and collected, to separate them from Ca and Sr. Subsequently, the Mg fraction was dried down in preparation for elution through a second column (also filled with BioRad X12 resin). For the second column pass, Mg was eluted using 1N HNO_3 and collected in order to achieve separation from Na and K. For the IC method, dissolved samples were dried down and redissolved in 0.2% HNO_3. The sample was then injected through a CS-16 cation exchange column and eluted with methanesulfonic acid (MSA). Mg fractions were collected using a Dionex AS-AP autosampler and yields were monitored through measurements of sample conductivity. Purified samples corresponding to 300-500 ng Mg were dried down in preparation for mass spectrometry.

Mass Spectrometry

In preparation for isotopic analysis, purified Mg samples were dried down and redissolved in 2% HNO_3. Samples were then diluted to a concentration of 150 ppb, either according to sample conductivity results from the IC, or by direct concentration checks on the MC-ICP-MS. Intensities of ^{24}Mg, ^{25}Mg, and ^{26}Mg were measured on the faraday cups L3, C, and H3, respectively. L3 and H3 are both three cups away from the center cup on either side. Measurements were conducted using a standard-sample-standard bracketing technique with Dead Sea Metal-3 (DSM3) - a pure Mg metal from the Dead Sea (Young and Galy, 2004). In addition to samples, the Mg isotope standard Cambridge-1, a Bermuda seawater standard, and an in-house dolomite standard were taken through the entire chemical procedure and measured with samples to assess accuracy and precision. We measured a value of -2.62 ± 0.15 ‰ (2σ SD; n = 8) for Cambridge-1 and a mean value of -0.84 ± 0.06 ‰ (2σ SD; n = 5) for Bermuda seawater. These values compare well with previously measured values of -2.58 ± 0.14 ‰ and -2.62 ± 0.25 ‰ for Cambridge-1 (Higgins and Schrag, 2010; Galy et al. 2003) and -0.82 ± 0.01 ‰ for

seawater (Foster et al. 2010). The external reproducibility of $\delta^{26}Mg$ from our in-house dolomite standard was ±0.11 ‰ (2σ SD, n = 8). We also measured the $\delta^{26}Mg$ of a modern *Porites* sp. coral (-1.87 ± 0.05 ‰; 2σ SD; n = 2), which is in agreement with values measured for other modern corals (Saenger et al. 2013; Wombacher et al. 2011). Mg intensities of samples and standards were monitored to ensure that concentrations were within 20% of each other. Triple-isotope plots of $\delta^{25/24}Mg$ vs. $\delta^{26/24}Mg$ were also examined for each run to check for mass-dependent behavior (see Fig. DR1).

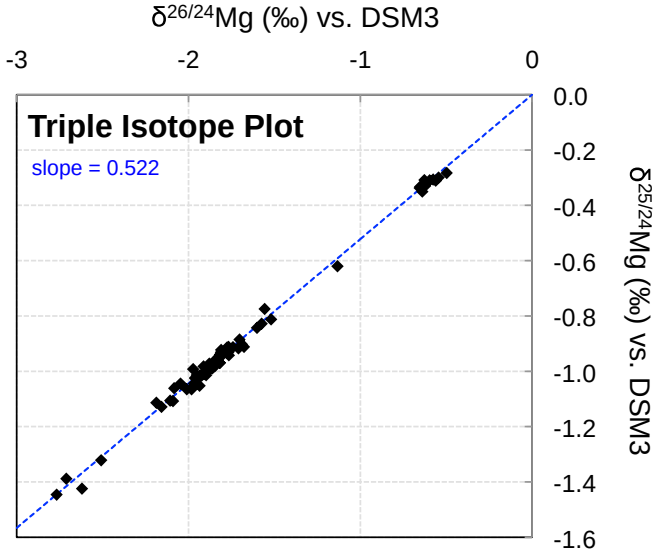

Figure DR1. Triple-isotope plot showing results of Mg isotope measurements. The slope of the $\delta^{26/24}Mg$ vs. $\delta^{25/24}Mg$ relationship is 0.522, consistent with the value reported in previous studies (Young and Galy, 2004; Husson et al. 2015).

MG ISOTOPE RESULTS:

Table DR1. Results of Mg isotope analyses for fossil corals.

Sample ID	Age (Myr)	$\delta^{26}Mg$[a]	2σ SD[b]
M1	0.0	-1.89	-
Pl3	0.1	-1.84	0.20
Pl5	0.1	-2.16	-
Pl2	1.4	-1.77	-
Pl7	2.0	-1.92	-
Pl8	2.2	-1.97	-
Pli3	2.3	-1.81	-
Pli2	3.1	-1.98	0.08
Pli1	3.5	-1.69	-
Mi6	5.4	-1.57	-
Mi11	9.3	-1.82	-
Mi7	14	-1.99	0.32
Mi1	18	-1.90	-
Mi3	18	-1.87	0.02
Ol1	29	-2.08	-
Ol4	30	-1.98	-

Ol5	30	-2.09	-
Ol6	30	-1.86	-
Ol3	32	-1.92	0.03
E6	35	-1.70	0.06
E8	36	-1.85	-
E2	37	-1.78	-
Ol2	38	-1.78	0.10
E1	38	-1.71	-
E4	45	-1.56	-
E3	50	-1.80	0.06
Pa2	56	-1.60	-
Pa1	60	-1.70	-
Pa3	62	-1.52	-
J1	160	-1.84	-

[a] Mg isotope composition relative to the standard DSM3 in ‰ notation.
[b] Standard deviation of replicate analyses from different analytical sessions. Samples for which no standard errors are reported were only measured once.

SIMS Mg/Ca AND ICP-MS Mg/Ca COMPARISON:

Gothmann et al. (2015) show that diagenesis can occur at a fine scale in fossil samples, and that microanalysis can be a useful way to ensure that small domains of altered material are avoided. Because the Mg isotope data presented in this paper come from bulk powders drilled from fossil coral hand samples, we measured Mg/Ca ratios in the same bulk powders analyzed for Mg isotopes to test whether small domains of diagenetic material enriched in secondary Mg might be biasing our results.

Aliquots of dissolved powders were measured for Mg/Ca ratios on Thermo Finnigan Element-2 Inductively Coupled Plasma Mass Spectrometer (ICP-MS). The Mg/Ca ratios of samples were determined using a set of matrix-matched in-house standards with Mg/Ca ratios spanning the sample range (Rosenthal et al. 1999). A carbonatite standard, OKA-II, was used to assess the accuracy and precision of our measurement. We measured a value of 4.75 mmol/mol for OKA-II ±6% 2σ SD – within uncertainty of the value reported by Gabitov et al. (2013) as measured by Isotope Dilution ICP-MS.

We find that Mg/Ca ratios measured on bulk powders by ICP-MS are generally compatible with ratios measured by SIMS. While there are many powder samples that disagree with the measured SIMS Mg/Ca ratio beyond our analytical uncertainty, these offsets are likely due to heterogeneity in Mg/Ca within coral samples. Indeed, the differences between SIMS Mg/Ca and bulk powder Mg/Ca data are within the range of Mg/Ca values measured within single coral using microanalysis techniques (e.g., Gagnon et al. 2007; Gothmann et al. 2015). In addition, they are within the range of values observed for bulk coral Mg/Ca for corals of similar geologic age. For example, a survey of Mg/Ca ratios in ~125 modern corals shows an average Mg/Ca ratio of 3.7 ± 1.1 mmol/mol (2s SD) (Gothmann et al. 2015, Supplementary Table EA16).

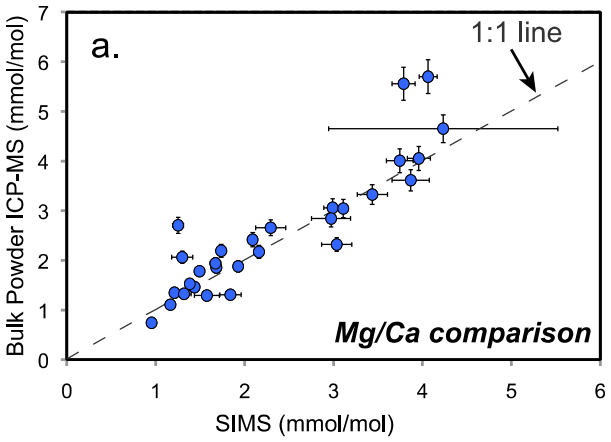

Figure DR2. Comparison of Mg/Ca measurements made on bulk powders by ICP-MS and by Secondary Ion Mass Spectrometry (SIMS). (a) Bulk powder measurements vs. average Mg/Ca ratios measured by SIMS. SIMS data are from Gothmann et al. (2015). Error bars for bulk powder ICP-MS data represent the external reproducibility based on repeat measurements of OKA-II - a carbonatite standard (~6% 2 S.D.). Error bars for SIMS data represent 2 S.E. of multiple SIMS spots measured within a single sample.

BOX MODEL OF SEAWATER [MG] and MG ISOTOPES:
To explore the relative importance of silicate and carbonate processes on the Cenozoic Mg cycle, we developed a simple 1-box model. Copies of the model are available from the authors upon request. The model is solved numerically in Matlab using ode23t, with model time steps of ~10,000 years, and is based on Equations 1-3 given in the main text.

The general model framework described above is used to generate Fig. 2 of the main text, as well as Figures DR3-DR5. The supplementary model figures all explore alternative scenarios and parameterizations to the model presented in Fig. 2 of the main text. However, the isotopic compositions and fractionation factors used are common between all model runs (see Table DR2 below). Initial conditions vary between the different model scenarios, and are presented in Table DR2. Information regarding model parameterizations for scenarios presented in Figures DR3-DR5 are given in the figure captions. Additional details regarding parameterizations for the model presented in Fig. 2 are given below.

Additional details regarding parameterizations of the model presented in Figure 2 of the main text: The model is parameterized such that both the flux of Mg to clays and dolomite have a first-order dependence on [Mg]sw. The Mg dolomite flux is also parameterized to have a dependence on global sea level as follows:

$$Fdol = (kdol * Mg_{SW}) * (1 + SL/A),$$

where Fdol has units of mol Mg/yr, kdol is a constant with units of (1/yr), Mg_{SW} is the inventory of Mg in seawater (mol Mg), SL is sea level in units of meters from the Miller et al. 2005 dataset, and *A* is a scaling factor in units of (1/m).

The silicate output flux does not explicitly separate removal of Mg during high-T basalt alteration, low-T basalt alteration, and authigenic clay formation. However, the value for the fractionation factor is chosen to be representative of these fluxes combined (see Table DR2).

Table DR2. Parameters and initial conditions chosen for the 1-box model of the Mg cycle used to generate Fig. DR3-DR5, and Fig. 2 of the main text.

Model Parameters	
Initial Conditions (Paleogene Seawater): Fig. 2 from main text	
Seawater [Mg]	30 mM[a]
River Mg Flux (Fcarb+Fsil)	(+) 4.5e12 mol/yr[b]
Silicate Mg Flux	(−) 3.6e12 mol/yr[c]
Dolomite Mg Flux	(−) 0.9e12 mol/yr[c]
Initial Conditions (Paleogene Seawater): constant dolomite flux (Fig. DR3a,b)	
Seawater [Mg]	30 mM[a]
River Mg Flux (Fcarb+Fsil)	(+) 4.5e12 mol/yr[b]
Silicate Mg Flux	(−) 3.7e12 mol/yr[c]
Dolomite Mg Flux	(−) 0.8e12 mol/yr[c]
Initial Conditions (Paleogene Seawater): constant clay flux (Fig. DR3c,d)	
Seawater [Mg]	30 mM[a]
River Mg Flux (Fcarb+Fsil)	(+) 4.5e12 mol/yr[b]
Silicate Mg Flux	(−) 1.05e12 mol/yr[c]
Dolomite Mg Flux	(−) 3.45e12 mol/yr[c]
Initial Conditions (Paleogene Seawater): Fig. DR4	
Seawater [Mg]	30 mM[a]
River Mg Flux (Fcarb+Fsil)	(+) 4.5e12 mol/yr[b]
Silicate Mg Flux	(−) 2.75e12 mol/yr[c]
Dolomite Mg Flux	(−) 1.75e12 mol/yr[c]
Initial Conditions (Paleogene Seawater): Fig. DR5	
Seawater [Mg]	30 mM[a]
River Mg Flux (Fcarb+Fsil)	(+) 4.5e12 mol/yr[b]
Silicate Mg Flux	(−) 1.05e12 mol/yr[c]
Dolomite Mg Flux	(−) 3.45e12 mol/yr[c]
Isotope Compositions/Fractionations (‰)	
Rivers (Carb+Sil)	-1.09[b]
SilicateClay (ε)	(−) 0.5[* d]
Dolomite (ε)	(+) 2.0[* d]
Additional Conditions	
Modern Seawater δ^{26}Mg	~-0.82 ‰[e]

* ε is defined as δsw - δsink, such that a negative ε results in a product that is heavier than seawater
[a] Chosen based on Zimmermann (2000), Horita et al. (2002), Lowenstein et al. (2003), Timofeeff et al. (2006)
[b] Chosen based on Wilkinson and Algeo (1989), Tipper et al. (2006), and Higgins and Schrag (2015)
[c] Chosen to fit the condition that Modern seawater $\delta^{26}Mg \approx -0.82$ ‰ vs. DSM3
[d] Chosen based on Higgins and Schrag (2010), Higgins and Schrag (2015), and Geske et al. (2015), and to fit data.
[e] From Galy et al. (2003)

MODEL CALCULATION OF MG ISOTOPE RESPONSE TO CHANGES IN CARBONATE/SILICATE MG CYCLING:

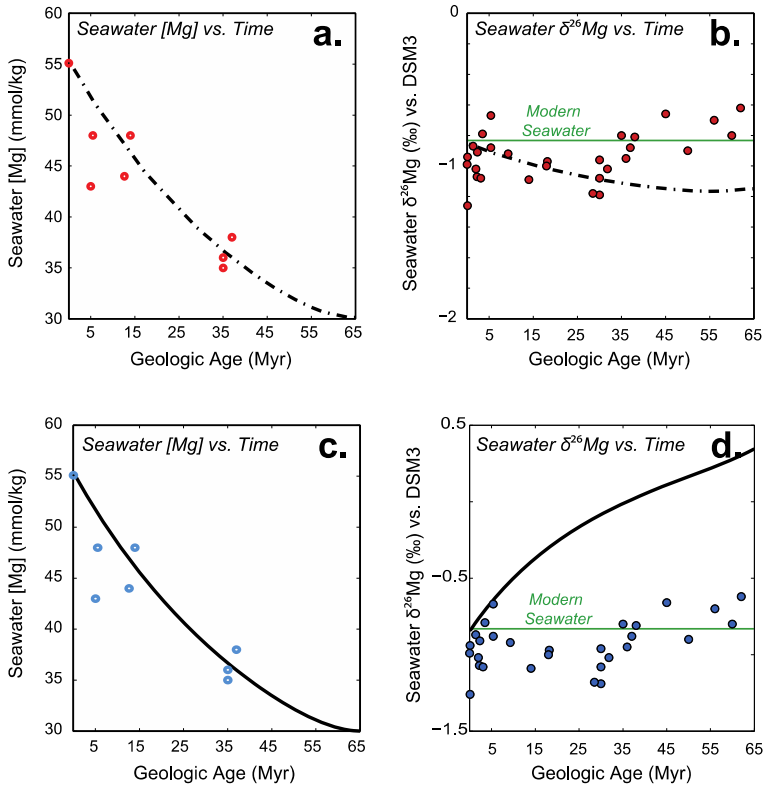

Figure DR3. Results of model calculations reproduced from Higgins and Schrag (2015). Figures show the magnitude of change in (a, c) seawater [Mg] and (b, d) seawater $\delta^{26}Mg$ that would result from driving secular variations in seawater [Mg] by invoking either (1) changes in Mg uptake in clay minerals (panels a and b with data shown in red), or (2) changes in dolomitization rates (panels c and d with data shown in blue). Seawater magnesium concentration data are taken from reconstructions from fluid inclusions trapped in halite and plotted in (a) and (b) along with model curves (Zimmermann, 2000; Horita et al., 2002; Timofeeff et al., 2006). Fossil coral Mg isotope data are shown in (b) and (d). The model (constructed following Eqns 1, 2, and Fig. 1 of the main text) is initially run to steady state. Then, the clay Mg sink, or the dolomite Mg sink is varied (while holding the other fluxes constant) to drive changes in seawater [Mg] consistent with fluid inclusion data. In addition, the $\delta^{26}Mg$ of Modern seawater in the model is required to match measured values of Modern seawater $\delta^{26}Mg$ (Galy et al., 2003), which is presented as a green line in (b) and (d). The plots convey that seawater $\delta^{26}Mg$ is

insensitive to changes in Mg uptake in clays, but responds to changes in dolomitization rates.

ALTERNATIVE MODEL PARAMETERIZATION TO FIG. 2 IN THE MAIN TEXT: NO DEPENDENCE OF DOLOMITE OUTPUT FLUX ON SEAWATER [MG]

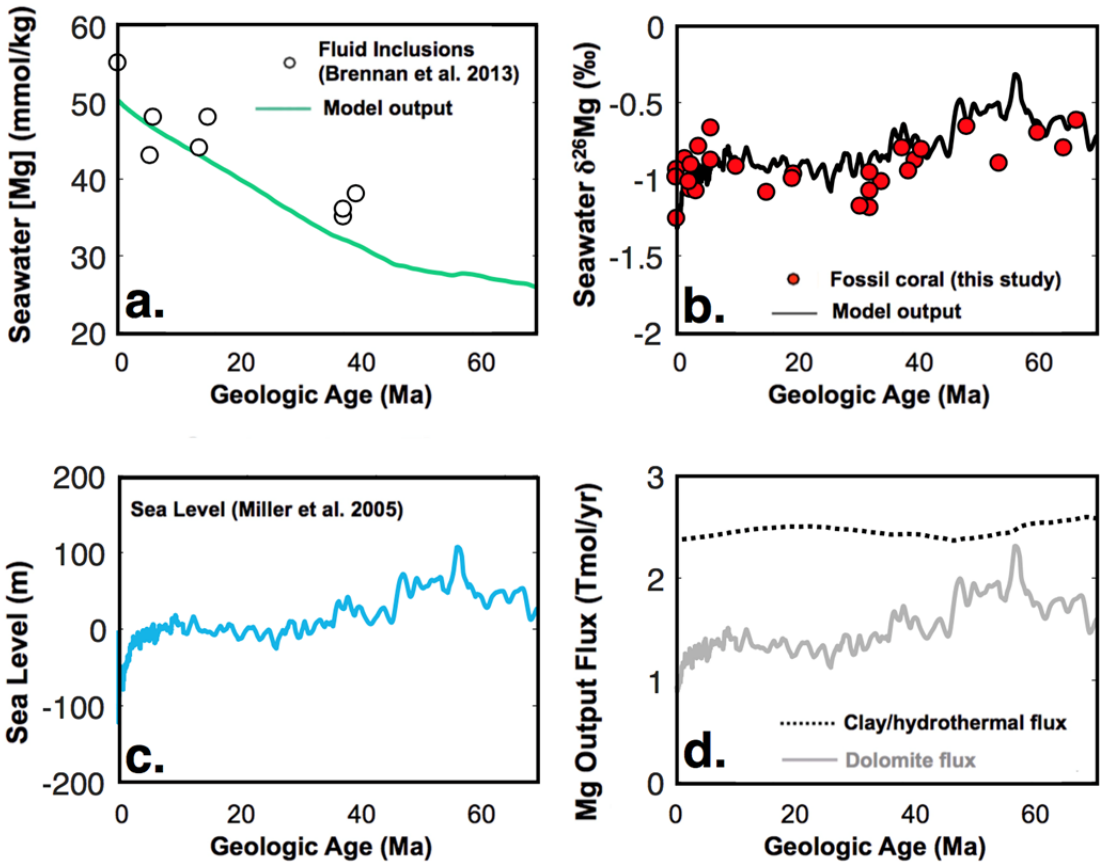

Figure DR4. Alternative parameterization for the model presented in Fig. 2 of the main text. The dolomite Mg output flux is parameterized to have a first-order dependence on sea-level as for Fig. 2, but there is no dependence of the dolomite flux on seawater Mg concentrations. In this case, Fdol =(kdol) * (1 + SL/*A*), where Fdol has units of mol Mg/yr, kdol is a constant with units of (mol Mg/yr), SL is sea level in units of meters from the Miller et al. 2005 dataset, and *A* is a scaling factor in units of (1/m). The silicate (clay/hydrothermal) Mg flux is parameterized to have a first-order dependence on seawater [Mg] (same as for the model presented in Fig. 2). In this model, the Mg output flux as dolomite is higher in the early Cenozoic as compared with the present, and the clay/hydrothermal Mg flux varies by <10%. While this model scenario appears to be consistent with seawater [Mg] reconstructions from fluid inclusions in halite (a), and while the shape of the modeled Mg isotope curve is similar to coral data, the modeled Mg isotopic composition in the early Cenozoic is heavier than observed by ~0.25 permil. While the fraction of Mg removed from seawater as dolomite does not change greatly during the last ~30 Ma, the total magnitude of the Mg sink is smaller than Mg sources

(rivers), which causes seawater [Mg] to increase toward the present.

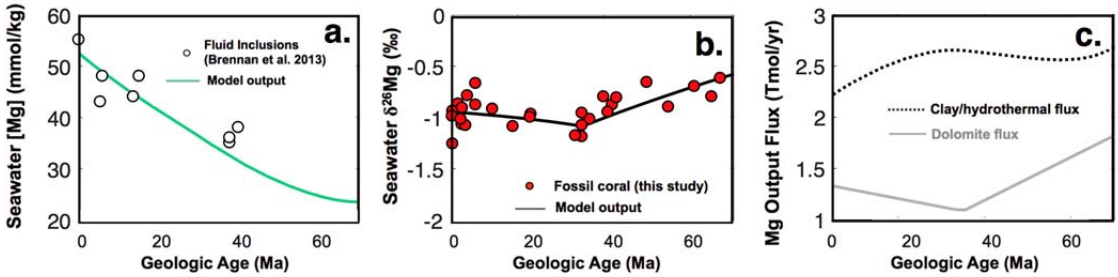

Figure DR5. Alternative model scenario where dolomitzation rates are prescribed to be higher in the early Cenozoic, but not dependent on sea level. The silicate (clay/hydrothermal) Mg flux is parameterized to have a first-order dependence on seawater [Mg]. In this model, the Mg output flux as dolomite is ~25% lower at 0 Ma than at ~65 Ma, and the clay/hydrothermal Mg output flux decreases by ~20% from ~30 Ma to the present. The seawater [Mg] rise is mainly driven by the decrease in the silicate (clay/hydrothermal) decrease between ~30 Ma and today.

REFERENCES:

Gabitov, R.I., Gagnon, A., Yunbin, G., Eiler, J., Adkins, J., 2013. Accurate Mg/Ca, Sr/Ca and Ba/Ca ratio measurements in carbonates by SIMS and NanoSIMS and an assessment of heterogeneity in common calcium carbonate standards: Chemical Geology, v. 356, p. 94-109.

Gagnon A. C., Adkins J. F., Fernandez D. P. and Robinson L. F. 2007. Sr/Ca and Mg/Ca vital effects correlated with skeletal architecture in a scleractinian deep-sea coral and the role of Rayleigh fractionation: Earth Planet. Sci. Lett. v. 261, p. 280–295.

Galy, A., Yoffe, O., Janney, P.E., Williams, R.W., Cloquet, C., Alard, O., Halicz, L., Wadhwa, M., Hutcheon, I.D., Ramon, E., Carignan, J., 2003. Magnesium isotope heterogeneity of the isotopic standard SRM980 and new reference materials for magnesium-isotope-ratio measurements: Journal of Analytical Atomic Spectrometry, v. 18, p. 1352-1356.

Geske, A., Goldstein, R.H., Mavromatis, V., Richter, D.K., Buhl, D., Kluge, T., John, C.M., Immenhauser, A., 2015. The magnesium isotope (δ^{26}Mg) signature of dolomites: Geochimica et Cosmochimica Acta, v. 149, p. 131-151.

Gothmann, A.M., Stolarski, J., Adkins, J.F., Dennis, K.J., Schrag, D.P., Schoene, B., Bender, M.L., 2015. Fossil corals as an archive of secular variations in seawater chemistry: Geochimica et Cosmochimica Acta, v. 160, p. 188-208.

Haq, B.U., Hardenbol, J., Vail, P.R., 1987. Chronology of Fluctuating Sea Levels Since the Triassic: Science, v. 235, p. 1156-1167.

Higgins, J.A., Schrag, D.P., 2010. Constraining magnesium cycling in marine sediments using magnesium isotopes: Geochimica et Cosmochimica Acta, v. 74, p. 5039-5053.

Higgins, J.A., Schrag, D.P., 2015. The Mg isotopic composition of Cenozoic seawater - evidence for a link between Mg-clays, seawater Mg/Ca, and climate: Earth and Planetary Science Letters, v. 416, p. 73-81.

Horita, J., Zimmermann, H., Holland, H.D., 2002. Chemical evolution of seawater during the Phanerozoic: implications from the record of marine evaporites: Geochimica et Cosmochimica Acta, v. 66, p. 3733-3756.

Husson, J.M., Higgins, J.A., Maloof, A.C., Schoene, B., 2015. Ca and Mg isotope constraints on the origin of Earth's deepest $\delta^{13}C$ excursion: Geochimica et Cosmochimica Acta, v. 160, p. 243-266.

Kominz, M.A., 1984. Ocean ridge volumes and sea-level change – an error analysis: American Association of Petroleum Geologists, p. 109-127.

Lowenstein, T.K., Hardie, L.A., Timofeeff, M.N., Demicco, R.V., 2003. Secular variation in seawater chemistry and the origin of calcium chloride basinal brines: Geology, v. 31, p. 857-860.

Miller, K. G., Kominz, M. A., Browning, J. V., Wright, J. D., Mountain, G. S., Katz, M. E., Sugarman, P. J., Cramer, B. S., Christie-Blick, N., and Pekar, S. F., 2005. The Phanerozoic record of global sea-level change: Science, v. 310, p. 1293–1298.

Müller, R. D., Sdrolias, M., Gaina, C., Steinberger, B., Heine, C., 2008. Long-term sea-level fluctuations driven by ocean basin dynamics: Science, v. 319, p. 1357– 1362.

Rosenthal, Y., Field, M.P., Sherrell, R.M., 1999. Precise Determination of Element/Calcium Ratios in Calcareous Samples Using Sector Field Inductively Coupled Plasma Mass Spectrometry: Analytical Chemistry, v. 71, p. 3248-3253.

Rowley, D.B., 2013. Sea Level: Earth's dominant elevation – implications for duration and magnitudes of sea level variations: Journal of Geology, v. 121, p. 445-454.

Timofeeff, M.N., Lowenstein, T.K., Martins da Silva, M.A., Harris, N.B., 2006. Secular variation in the major-ion chemistry of seawater: Evidence from fluid inclusions in Cretaceous halites: Geochimica et Cosmochimica Acta, v. 70, p. 1977-1994.

Tipper, E.T., Galy, A., Gaillardet, J., Bickle, M.J., Elderfield, H., Carder, E., 2006. The magnesium isotope budget of the modern ocean: Constraints from riverine magnesium isotope ratios: Earth and Planetary Science Letters, v. 250, p. 241-253.

Wilkinson, B.H., Algeo, T.J., 1989. Sedimentary carbonate record of calcium and magnesium cycling: American Journal of Science, v. 289, p. 1158-1194.

Young, E.D., Galy, A., 2004. The Isotope Geochemistry and Cosmochemistry of Magnesium: Reviews in Mineralogy and Geochemistry, v. 55, p. 197-230.

Zimmermann, H., 2000. Tertiary seawater chemistry - Implications from fluid inclusions in primary marine halite: American Journal of Science, v. 300, p. 723-767.